Materials and Design 203 (2021) 109624

Contents lists available at ScienceDirect

Materials and Design

journal homepage: www.elsevier.com/locate/matdes

Mechanical properties of 3D printed mouthguards: Influence of layer height and device thickness

Ana M. Sousa, Ana C. Pinho, Ana P. Piedade *

University of Coimbra, CEMMPRE, Department of Mechanical Engineering, 3030-788 Coimbra, Portugal

HIGHLIGHTS

- Evaluation of the potential of polymeric materials, other than EVA, for the production of 3D printed mouthguards.
- Test specimens were printed using commercial filaments of rPLA, PMMA, HIPS and TPU.
- The influence of the printing quality (layer height) and total thickness in the properties/characteristics was specifically studied.
- The mechanical properties were determined: filaments through tensile tests and printed materials by three-point bending and transversal impact tests.

GRAPHICAL ABSTRACT

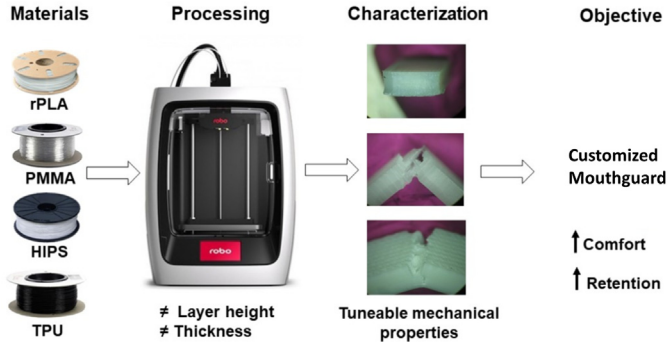

ARTICLE INFO

Article history:
Received 26 September 2020
Received in revised form 12 February 2021
Accepted 27 February 2021
Available online 3 March 2021

Keywords:
Mouthguards
Polymer
Additive manufacturing
Device thickness
Energy absorption

ABSTRACT

Mouthguards are polymeric devices recommended to be used by athletes to help prevent orofacial injuries. Some of the problems described by the athletes when using the mouthguards can be addressed by producing customized devices with thinner walls by additive processing techniques.

In the present work, new polymeric materials for this application, such as poly(lactic acid) (rPLA) recycled from food packaging, poly(methyl methacrylate) (PMMA), high impact polystyrene (HIPS), and thermoplastic polyurethane (TPU), are proposed for the preparation of protective mouthguards, in alternative to the ethylene-vinyl acetate (EVA) copolymer, the current gold standard. Specimens were printed with two different thicknesses (2 mm and 4 mm) to study their influence on the final properties of the printed samples. The characterization included chemical, thermal, surface, and mechanical aspects of commercially acquired polymeric filaments and printed components.

All the studied materials showed a decrease in the impact strength with increasing specimen thickness, except for TPU due to its highest deformation capacity. Compared with EVA, TPU has a similar energy absorption, while the other polymers presented higher values.

1. Introduction

When exposed to impacts resulting from physical activity, athletes are more prompt to suffer orofacial injuries. They represent 18% of all sports trauma, and 50% are directly related to dental disturbance [1]. To prevent this type of injury, the use of mouthguards was proved to be useful. For this reason, in 1960, the American Dental Association (ADA) implemented the mandatory use of mouthguards in sports with a high physical impact, such as wrestling, American football, and hockey, among others [2].

* Corresponding author.
E-mail address: ana.piedade@dem.uc.pt (A.P. Piedade).

https://doi.org/10.1016/j.matdes.2021.109624

Protective mouthguards are devices that intend to absorb and dissipate the impact energy resulting from physical contact during sports activity, both for training and competition [3]. Since they are meant to be placed inside the mouth next to the dental arch, it is essential that the device is comfortable to wear and does not interfere with the physical performance of the athlete [4,5]. Therefore, several aspects must be taken into consideration in the design of these devices. Several surveys made to athletes revealed that the main reason they do not like to use or do not use it is the discomfort and the impairment in breathing that the devices provoke, mostly due to their thickness [6]. So, the athlete is more concerned with comfort than with prevention, especially considering that their athletic performance also decreases due to the discomfort and sometimes pain felt during the use of the mouth protectors [7].

The material used in the mouthguards must be biocompatible, non-toxic, and insipid [8]. It should also be able to absorb, but mostly dissipate, the impact energy resulting from the physical contact by redistributing the impact forces over a larger area and, therefore, decreasing the probability of orofacial injury or failure of the protective device [9]. Other important properties to consider are stiffness, hardness, and the swelling behavior of the material. Furthermore, the mechanical properties of the materials used to produce mouthguards should be evaluated, not only after processing but also in its swollen state, since it will be used in a moist environment [10].

Since most mouthguards are designed to be placed on the upper jaw, it is paramount to achieve a correct adjustment and guarantee retention [11]. The thickness of the device is also of great importance as it influences the final retention, which affects the athlete's physical performance [12]. Nowadays, there are three different designs of mouthguards according to ASTM F697–16 – "Standard practice for care and use of athlete mouth protectors". However, the attributed classification is not the most used in both sports and scientific areas. Instead, the devices are classified according to the manufacturing process as stock, "boil and bite," and custom-made mouthguards [13].

Stock mouthguards present the most basic design having a flat surface with no customized adjustment to the dental arch. This design results in low retention and comfort, as reported in the literature [4]. Therefore, since they are relatively cheap compared to the other types, they are often used as a substitute device or orthodontic treatment [8].

Although having a flat design, the "boil and bite" mouthguards allow the imprinting of the dental arch by heating the device in hot water and, after placed inside the mouth, biting the device to adjust it to the mouth arch [14]. This procedure increases the retention of the mouthguard and the comfort of the athlete. Although they represent an upgrade compared to the stock devices, achieving a perfect dental arch print is not always possible. The "boil and bite" are the most used type of protectors as their cost is quite accessible.

Finally, the custom-made mouthguards are the most recommended by health professionals as they are created from the individual mold of the dental arch of the final user [15]. Besides providing the best fit, these mouthguards are also more effective in protecting and more comfortable to wear [16,17]. However, since they are customized, their cost is much higher.

There are two conventional processing techniques for fabricating custom-made mouthguards known as pressure and vacuum thermoforming. Both are based on the conformation of one or more sheets after pre-heating the thermoplastic polymer [8]. After reaching the ideal temperature, the material is forced towards the mold by pressure or vacuum action. When the correct coverage of the mold is achieved, the thermoplastic polymer is cooled, and the imperfections trimmed. Although these techniques are widely used, they both need an individual pre-fabricated mold of the dental arch, which increases the fabrication cost and time. Moreover, they produce waste as the polymeric sheets are not entirely used.

Considering the material for mouthguards manufacture, ethylene-vinyl acetate (EVA) copolymer is the gold standard, mostly due to its processability and shock absorption capacity. However, EVA presents some limitations related to high swelling capacity and low rigidity, leading to dimensional variation and insufficient shock energy dissipation, respectively. Also, some problems related to surface roughness and microorganisms adhesion have been reported [18].

Despite what is already reported in the literature, the ideal mouth guard is yet to be created. Both the manufacturing methods and the polymeric material present some limitations. Moreover, most of the reported published research is from the Dentistry scientific area, which implies that they aim to study the medical consequences of using commercial mouthguards and not from the Materials perspective. Consequently, issues like testing new materials, new processing techniques, and new designs are almost absent from the published work.

The present work intends to address these limitations, evaluating the possibility of manufacturing mouthguards using 3D printing since it allows producing complex and completely personalized shapes without the need for a mold. Also, the study of other polymeric materials intends to evaluate the possibility of substituting EVA. The optimization of the thickness of the mouthguards is also discussed, aiming at enhancing comfort without compromising the protection.

2. Materials and methods

2.1. Materials

Recycled poly(lactic acid) (rPLA) filament was purchased from Refil®, Rotterdam, Netherlands, while high impact polystyrene (HIPS) filament was obtained from DoWire®, Seixal, Portugal. Both poly (methyl methacrylate) and thermoplastic polyurethane (TPU) filaments were acquired from TreeD Filaments™, Seregno, Italy. All filaments had a diameter of 1.75 mm, were used as received and presented a purity higher than 98%. The filaments were characterized in terms of chemical composition, thermal behavior, and mechanical properties, as described in the next sub-sections.

2.2. Processing technology

All testing specimens were prepared by 3D printing using a 3D Robo R2 printer equipped with a 0.4 mm diameter nozzle. It must be mentioned that the used 3D printer has a close chamber, which allows a constant temperature throughout each printing cycle precisely at the same environment temperature as the previous one. A series of preliminary studies were made in order to optimize the printing parameters. One variable parameter considered in this study was the layer height, where two distinct values were tested: a layer height of 0.2 mm (LQ) and a layer height of 0.1 mm (NQ). Also, the total thickness of the specimens was varied and their impact on the final properties/characteristics of the printed specimens evaluated. Final thicknesses of 2 and 4 mm were considered (Table 1). The printing and bed temperatures were adjusted according to each filament (after thermal characterization). Both the geometry and size of the printed specimens varied according to the requirements of each characterization technique, as

Table 1
Some of the constant and variable printing parameters.

Filament	$T_{printing}$ (°C)	T_{bed} (°C)	P_v (mm/s)	Quality
rPLA	195	60	50	LQ
				NQ
PMMA	220	70	50	LQ
				NQ
HIPS	220	70	50	LQ
				NQ
TPU	220	30	35	LQ
				NQ

T = temperature; P_v = printing velocity.

specified in the next sections. For each characterization technique, six specimens were printed.

2.3. Characterization techniques

Due to the lack of information regarding the properties/characteristics of the purchased filaments, the chemical, thermal and mechanical properties were evaluated. The results also provided information that helped decide the range of printing parameters used in the preliminary experiences to optimize the 3D printing process.

2.3.1. Chemical characterization

The chemical analysis of the filaments was made by Fourier transform infrared spectroscopy (FTIR), using the attenuated total reflectance (ATR) sampling technique. The infrared spectrum of each solid sample was recorded at 20 °C, using a Perkin Elmer Frontier spectrometer (FTNIR/MIR), equipped with an FR-DTGS detector and a KBr beam splitter. Spectrum registration was performed with 4.0 cm^{-1} resolution with 64 accumulations. A Perkin Elmer sampling accessory, universal ATR module (UATR Universal Attenuated Total Reflectance), with diamond crystal/ZnSe, was used, and a constant 80 N force was applied during all acquisitions.

2.3.2. Thermal characterization

The thermal stability of the filaments was evaluated by thermal gravimetric analysis (TGA) using a TGA Q500 V20.13 equipment, at a heating rate of 10 °C/min, from 25 to 600 °C, under a nitrogen flow of 50 mL/min. Differential scanning calorimetry (DSC) was also used to determine the thermal events. Measurements were carried out on a DSC Q100 V9.9 equipment from TA instruments, with a scan rate of 10 °C/min, from −70 to 300 °C, under a nitrogen flow of 50 mL/min. The crystallinity (χ_c) of rPLA was calculated using eq. (1) [19],

$$\chi_c(\%) = \frac{\Delta H_m - \Delta H_{cc}}{\Delta H_\infty} \times 100 \quad (1)$$

where ΔH_m is the variation of enthalpy associated with the melting, ΔH_{cc} is the variation of the cold crystallization enthalpy and ΔH_∞, which is assumed to be 93.1 $J.g^{-1}$, is the variation of enthalpy for the melting of a theoretical 100% crystalline PLA [19].

2.3.3. Mechanical characterization

The mechanical characterization of the filaments was assessed by tensile tests because the materials experience tensile forces when being extruded through the printer nozzle. A Shimadzu Autograph AGS-X equipped with a 5 kN load cell, with a grip speed of 5 mm/min at room temperature, was used. Five samples were tested for each material and a distance between grips (L_0) of 50–65 mm.

2.3.4. Surface characterization of the printed specimens

The surface topography of the printed specimens was assessed by Infinite focus microscopy (IFM) using an Alicone Infinite Focus G4 profilometer equipped with a fixing sample system. The surface roughness parameters S_a (surface area average height), S_q (surface area root-mean-square height), and the true to projected surface area ratio (r factor) were determined.

The wettability of the printed materials was assessed by the measurement of the static contact angle of distilled water and formamide at room temperature, using an OCA20 Dataphysics Instruments GmbH apparatus. Five drops (10 μL) were deposited in each sample, and the contact angles were taken after the system air-water-surface reached the equilibrium. The calculation of the apparent contact angle values (θ_a) was obtained using five measurements for each material and printing quality. The correction for the roughness of the θ_a values was performed according to the Wenzel's equation (Eq. (2)),

$$cos\theta_a = r \times cos\theta_r \quad (2)$$

where r is the true to projected area ratio (r factor - roughness parameter), and θ_r is the contact angle for a smooth surface [20]. The r factor value was determined by IFM, as previously described. All the surface energy calculations were performed using the corrected contact angle values (θ_r). The determination of the surface energy was performed by using the contact angle values. The total surface energy (γ_s) is obtained by the sum of the dispersive (γ_s^d) and polar (γ_s^p) components [21]. All calculations were conducted following the methodology previously described [22].

2.3.5. Mechanical characterization of the printed specimens

Three-point bending (3 PB) tests were conducted according to the ASTM Standard D 790 recommendations. Specimens with 60 × 10 × 2 mm and 90 × 10 × 4 mm. Six specimens of each material, layer height, and final thickness of 2 or 4 mm were tested using a Shimadzu AG-10 universal testing machine equipped with a 5 kN load cell at room temperature, with a grip speed of 2 mm/min. The bending strength was calculated as the nominal stress in the middle span section obtained using the maximum value of the load. The nominal bending stress was calculated using according to Eq. (3):

$$\sigma = \frac{3PL}{2bh^2} \quad (3)$$

where P is the load, L the span length, b the width and h the thickness of the specimen [23]. The Young's modulus was calculated by the linear elastic bending beams theory relationship, according to Eq. (4),

$$E = \frac{\Delta P L^3}{48 \Delta \mu I} \quad (4)$$

where I is the moment of inertia of the cross-section and ΔP and $\Delta \mu$ are, respectively, the load range and flexural displacement range, in the middle span, for the interval of the linear region of the load *versus* displacement plot [24]. The Young's modulus was obtained by linear regression of the load-displacement curves considering the interval in the linear segment with a correlation factor greater than 95%. All results are presented as the mean ± standard deviation of the mean value.

Transverse impact tests were carried out according to ISO 179 Charpy Impact. Six specimens of two different sizes (80x10x2 and 80x10x4 mm) with a 1 mm V shape notch, for each material and printing quality, were tested, at room temperature, using an impact machine Instron-Ceast 9050 with a 5 J hammer. Control samples of bulk EVA ((80x10x4) from Dentaflux, Madrid, Spain) were tested using the same equipment and conditions. The damage morphology was observed with the help of a Stemi 2000-c (Carl Zeiss) magnifying glass with 5× amplification and images recorded with a Powershot G5 camera, by Canon, with 16× amplification. Some of the fractured materials were also observed by Scanning Electron Microscopy (SEM) aftet coating the surface with 30 nm sputtered gold. Six specimens of each size, material, and layer height were tested, and the results are presented as the mean ± standard deviation of the mean value.

Considering the application for mouthguards and the mechanical solicitations that they will endure, tensile tests were not used for characterizing the mechanical properties of the printed specimens.

3. Results and discussion

3.1. Filaments

For the preparation of the printed testing specimens, four different polymeric filaments were used as received. Their characterization before the processing step will now be discussed. This set of characterizations is

needed because the commercially purchased filaments do not give any information.

3.1.1. Chemical characterization

FTIR assessed the identification of the characteristic chemical functional groups of each polymer, and Fig. 1 presents the FTIR spectra of each filament.

All filaments present the typical bands expected for each type of polymer, confirming their fingerprint. In the case of PLA, it was possible to identify the stretching frequencies of the following groups: O—H (a) at 3700–3500 cm^{-1} [24], CH_3 (b) at 2945 cm^{-1} [25] and C═O (c) at 1751 cm^{-1} [24]. The PMMA spectrum shows the bands corresponding to the stretching vibration of CH_3 (d) at 2995 cm^{-1} [26], the asymmetric and symmetric stretching of CH_2 (e) at 2950 cm^{-1} [27], the stretching vibration of the C═O from the ester linkage (f) at 1720 cm^{-1} [28] and the stretching vibration of C-O-C (g) at 1144 cm^{-1} [26]. In turn, the HIPS spectrum shows the presence of the stretching vibration of C═C (h) and C—H (i) groups, from the benzene rings, at 1600 cm^{-1} [29] and 753–694 cm^{-1} [30], respectively. Finally, concerning the TPU spectrum, it shows the stretching vibrations of the following groups: N—H (j) at 3335 cm^{-1} [31], C═O (k) from the urethane linkage at 1725–1701 cm^{-1} [27], and C—N (k) at 1308 cm^{-1} [32]. No significant differences were found in any spectra in comparison to what is reported in the literature. Therefore, it can be assumed that the eventual presence of additives does not induce considerable changes in the chemical composition of the filaments.

3.1.2. Thermal characterization

TGA assessed the thermal stability of the materials for a temperature range between 25 and 600 °C. The obtained thermogravimetric curves and respective derivatives (TGA and DTG) are plotted in Fig. 2.

The decomposition of rPLA occurs mainly in one stage between 250 and 400 °C, as reported in the literature [33]. However, a second stage can be observed between 410 and 470 °C, which might be assigned to the degradation of larger PLA chains. The broad DTG curve confirms a large distribution of the molecular weight of the macromolecules. According to what is systematically described in the literature, this result is attributed to the mechanical recycling process, where the applied shredding forces lead to the break of the chemical bonds of the main polymeric chain [34]. This action provokes a broader distribution of polymeric chain sizes and, consequently, a larger distribution of molecular weights.

With the increase in recycling cycles, the average molecular weight tends to decrease due to chain scission [34]. Concerning PMMA and HIPS, they present one single stage of degradation between 285 and 400 °C and 370–485 °C, respectively. These results are in agreement with the typical ranges reported for these polymeric materials [35,36]. Finally, the degradation of TPU occurs in two different weight loss stages. The first, between 250 and 380 °C, is ascribed to the decomposition of the urethane bond, while the second (380–540 °C) corresponds to the degradation of the polyol chains [37]. Table 2 summarizes the temperatures of interest obtained from the thermogravimetric curves.

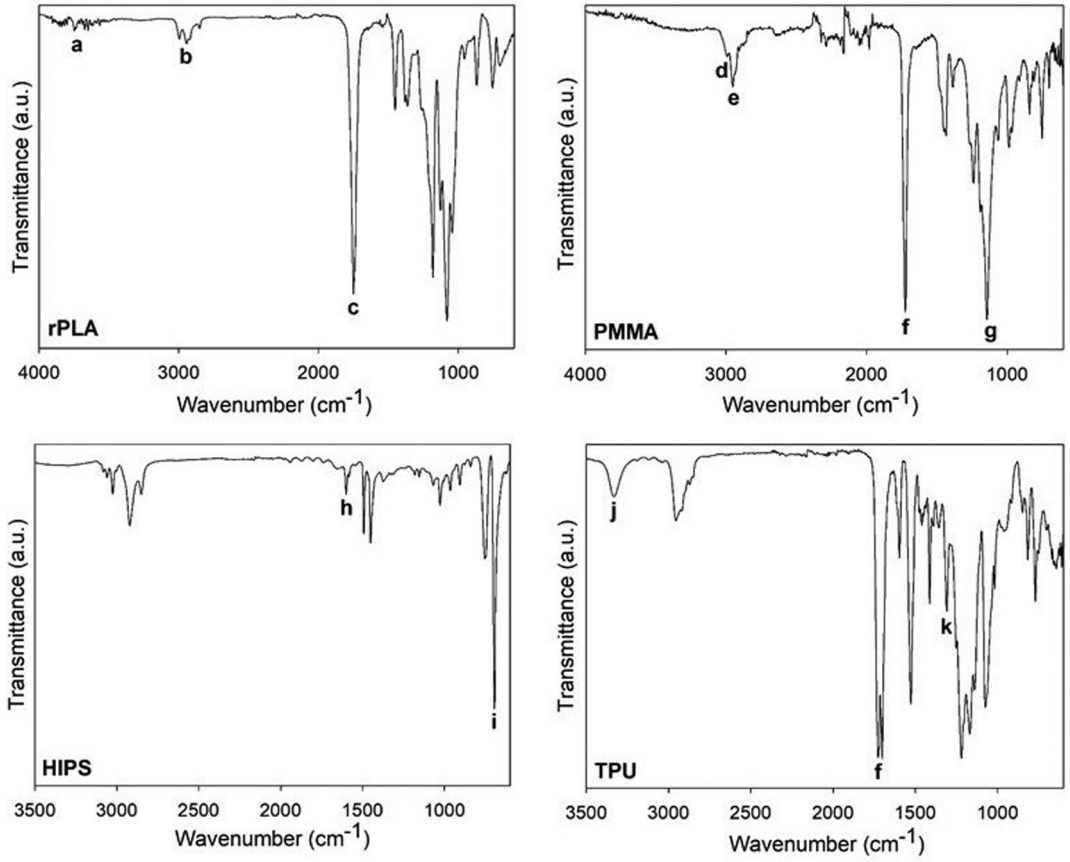

Fig. 1. FTIR spectra of rPLA, PMMA, HIPS and TPU filaments.

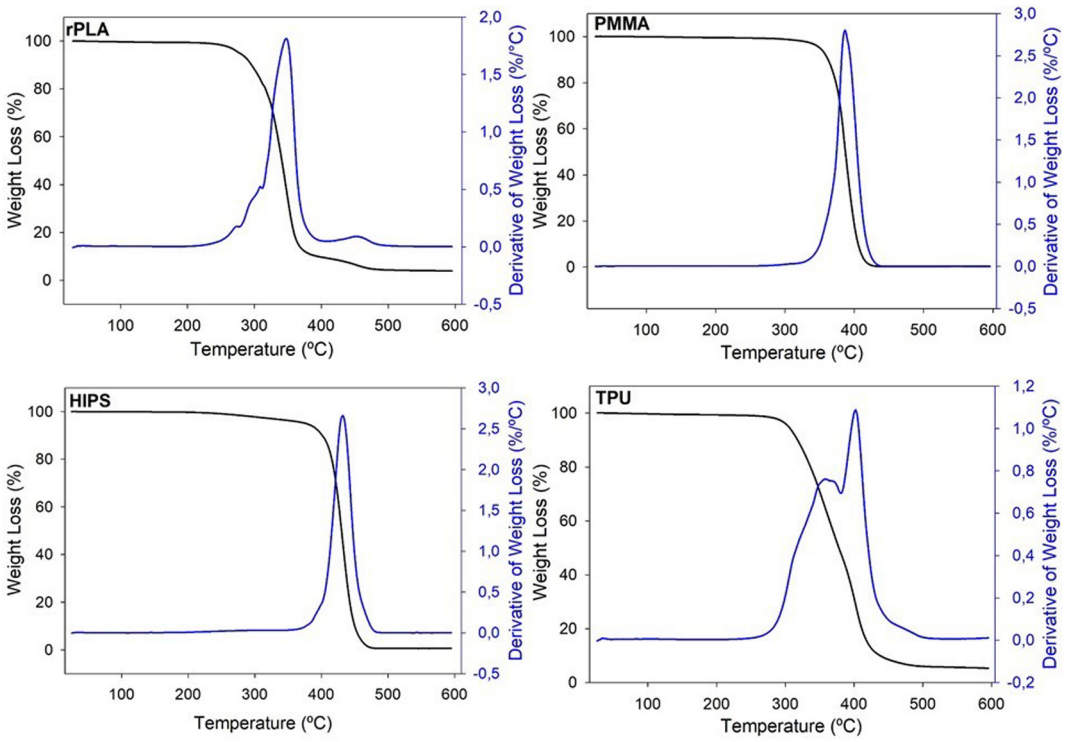

Fig. 2. Thermogravimetric curves of rPLA, PMMA, HIPS and TPU filaments.

Table 2
Characteristic temperatures determined by TGA, where T_{on} is the onset temperature; $T_{5\%}$ stands for the temperature that corresponds to 5% of weight loss; $T_{10\%}$ is the temperature at 10% of weight loss and T_p is the peak temperature.

Filament	T_{on} (°C)	$T_{5\%}$ (°C)	$T_{10\%}$ (°C)	$T_{p,1}$ (°C)	$T_{p,2}$ (°C)
rPLA	313.6	277.7	295.8	347.5	–
PMMA	370.8	350.5	362.2	386.6	–
HIPS	411.9	376.9	401.4	432.1	–
TPU	332.0	304.6	317.8	402.3	358.4

Table 3
Mechanical properties of the filaments, where P is the maximum applied load, σ is the tensile strength and ε is the strain at break.

Filament	P (N)	σ (MPa)	ε (%)
rPLA	83 ± 14	35 ± 6	20 ± 22
PMMA	82 ± 7	34 ± 3	10 ± 3
HIPS	15 ± 2	5 ± 1	38 ± 6
TPU	20 ± 0	8 ± 0*	266 ± 17*

* Value at 20 N load.

According to the obtained results, it is possible to conclude that all polymeric materials are thermally stable until *ca.* 300 °C. Indeed, HIPS is the most stable filament, being able to resist temperatures close to 400 °C. Despite the slight differences observed in the temperature values obtained in our experiments compared with the literature, it can be assumed that the processing steps required towards the filament conformation do not significantly influence the thermal stability of the polymeric materials.

The thermal events of the polymeric materials were studied using the DSC technique. The rPLA filament presents three different events that are ascribed to the glass transition (T_g) at 59.4 °C, the melting temperature (T_m) at 171.0 °C, and cold crystallization (T_{cc}) at 98.3 °C. The cold crystallization enthalpy (ΔH_{cc}), also determined from the heat flow curve, is 26.3 J/g. In addition to these values, the crystallinity percentage (χ_c) was calculated to be 8.7%. On the other hand, both PMMA and HIPS only show one single event assigned to the T_g (113.5 °C and 99.0 °C, respectively) characteristics of amorphous structure. In the case of TPU, two glass transition temperatures can be identified. According to the literature, this behavior is due to the broad polymeric chain distribution. Herein, the longer chains or soft segments are the polyol-diisocyanate chains, while the smallest chains or hard segments are created between the boundaries of the diisocyanates and short diol chains [38]. Therefore, the first T_g ($T_{g1} = -21.4$ °C) refers to the soft segments, and the second T_g ($T_{g2} = 66.9$ °C) corresponds to the hard segments.

3.1.3. Mechanical characterization

The mechanical properties of the filaments were studied through stress-strain curves obtained from the tensile tests. For the filaments rPLA, PMMA and HIPS, all tests were performed until total rupture. In TPU, the tests were interrupted at a maximum load of 20 N due to their extreme deformation (Table 3).

The results show that regardless of the similar tensile strength of rPLA and PMMA, for the same load values, PMMA presents lower strain values. However, rPLA reveals higher dispersion of results, which can be a consequence of the recycling process that induces a broad distribution of molecular weights, as already discussed. Nevertheless, HIPS presents the highest strain and lower tensile strength, at rupture, between the three filaments. Since the TPU tests were not completed until rupture, its results cannot be directly compared with the other materials. As can be seen in Table 3, the strain value obtained for a 20 N load is much higher than the other filaments. These results agree to what was expected, as this material presents high ductility, which means that even for lower loads, it presents high strain values.

3.2. Printed specimens

3.2.1. Thermal characterization

TGA and DSC thermally characterized the printed specimens to evaluate if the printing process affected the thermal properties. The TGA

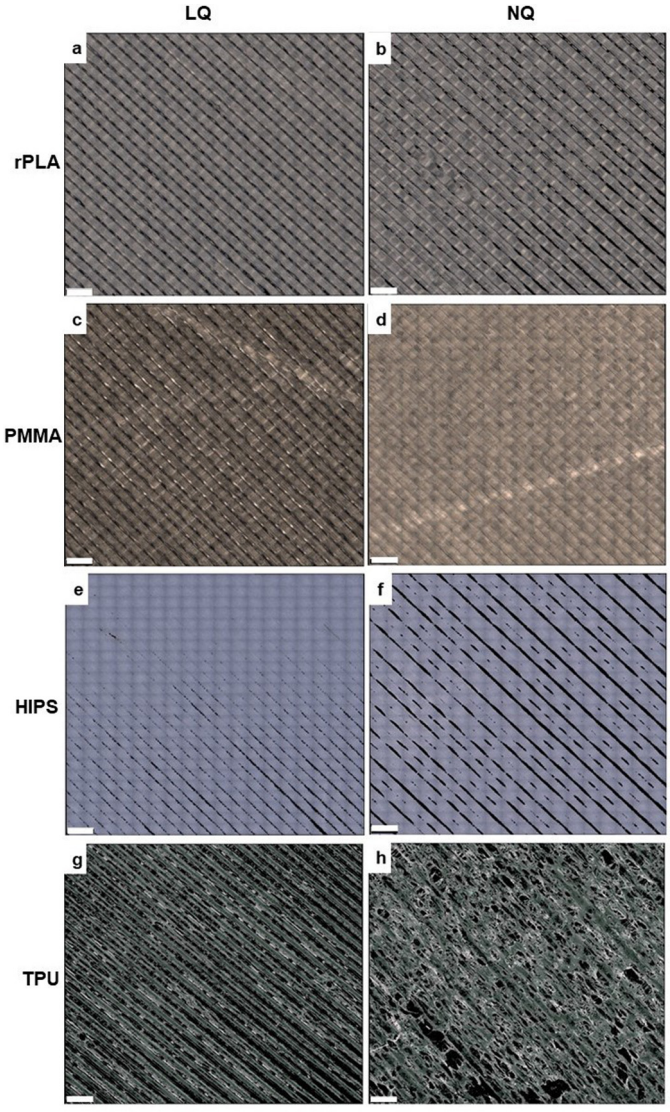

Fig. 3. Reconstructed surface micrographs obtained by IGM of the printed samples (scale bar = 1 mm). Inserts correspond to average surface roughness values.

analysis showed no differences between the processed polymers and the filaments. Also, the thermal events registered in the DSC analysis indicated no relevant changes, with the values of T_g, T_{cc}, and T_m varying within the error associated with the equipment.

3.2.2. Surface characterization

IFM evaluated the topography and roughness parameters of the surface of the printed samples. Fig. 3 shows the obtained representative micrographs of the surface of the samples printed in LQ and NQ for each material, with 2 mm of the total thickness.

Besides the topographic images, the same technique also allowed to determine some surface roughness parameters and the *r* factor (Table 4).

Considering the obtained results, TPU shows the highest average roughness values, which can be confirmed by the observation of Fig. 3, and results from Table 4 inserted in the micrographs, where it is evident that the TPU surfaces are less smooth, regardless of the layer height. In contrast, HIPS presents the lowest roughness values, followed by rPLA.

For PMMA, it can be pointed out that the printing parameters significantly influence the roughness parameters. When PMMA was printed in NQ, the average roughness almost doubled. On the contrary, for TPU the decrease of layer height had the opposite effect as the average roughness in inferior for NQ. In both HIPS and rPLA, the layer height did not significantly influence the roughness parameters.

The measurement of the static contact angles allowed to classify the hydrophilicity ($\theta_{water} \leq 65°$) or hydrophobicity ($\theta_{water} > 65°$) of the printed samples [39]. It is an established fact that the surface roughness influences the contact angle [21]. Thus, there was a need to correct the contact angle obtained directly by using the *r* factor. Table 5 summarizes the corrected contact angles (θ_r) determined for the different surfaces in contact with distilled water and formamide.

Considering the values presented in Table 5, all surfaces are considered hydrophobic. Herein, it is also possible to conclude that the layer height did not influence the wettability of the materials. These results were expected considering that the chemical composition is the same, and the values are corrected given the surface roughness. From all studied surfaces, TPU is the one presenting the most accentuated hydrophobic character. The surface reactivity of each polymer was determined by calculating their surface energy (γ_s), and the results are presented in Table 6.

The study of the surface energy of materials is of extreme importance as it helps to predict and understand the behavior of a surface when exposed to body fluids [39], which is particularly important for the envisaged application as mouthguards. In the present work, since all materials are polymers, they have low surface energy values, as expected [40].

Considering the layer height that reflects on the printing quality, it can be assumed that this parameter influences the surface energy in all materials except for TPU. In rPLA and PMMA, an increase of surface energy is observed for the samples printed in NQ. On the other hand, the opposite is observed for HIPS since the surface energy decreases with the layer height. Therefore, the interaction between the HIPS surface and the surrounding media will not be as facilitated as for the other samples, especially in the NQ printed samples. The polar and dispersive components of the surface energy are also quite important in evaluating the reactivity of a surface with water. Several authors state that the higher the polar component value, the highest the reactivity with water will be [39].

Table 4
Roughness parameters of the printed samples.

Materials	Quality	S_a (μm)	S_q (μm)	*r* factor
rPLA	LQ	11.7	15.1	1.061
	NQ	11.2	18.0	1.094
PMMA	LQ	20.4	26.2	1.100
	NQ	10.0	13.5	1.014
HIPS	LQ	7.8	10.3	1.067
	NQ	7.9	10.2	1.072
TPU	LQ	38.2	48.9	1.681
	NQ	22.1	31.8	1.737

Table 5
Corrected average contact angle values of the studied surfaces in contact with distilled water and formamide.

		Distilled water	Formamide
Material	Layer height	θ_r (°)	θ_r (°)
rPLA	LQ	89 ± 4	63 ± 7
	NQ	88 ± 2	62 ± 4
PMMA	LQ	89 ± 6	71 ± 6
	NQ	82 ± 6	62 ± 4
HIPS	LQ	99 ± 10	77 ± 3
	NQ	93 ± 3	75 ± 6
TPU	LQ	105 ± 4	87 ± 5
	NQ	98 ± 6	82 ± 7

Table 6
Calculated surface energy and respective polar and dispersive components.

Material	Quality	$\gamma_S\ (mJ.m^{-2})$	$\gamma_S^p\ (mJ.m^{-2})$	$\gamma_S^d\ (mJ.m^{-2})$
rPLA	LQ	37.8	1.6	36.2
	NQ	39.5	1.6	37.9
PMMA	LQ	28.3	3.8	24.5
	NQ	32.2	6.1	26.1
HIPS	LQ	27.6	0.7	26.9
	NQ	25.1	3.1	22.0
TPU	LQ	31.6	0.6	31.0
	NQ	31.6	0.03	31.6

In the case of the studied materials in the present work, the polar component is inferior to the dispersive component, which confirms that these polymeric surfaces are less likely to interact with the mouth fluids of the athletes. The combination of low reactivity, low polar component, and hydrophobic character may minimize the hydrolytic degradation and the bacterial growth on the devices printed with these materials. When considering only the surface characteristic/properties, it can be assumed that HIPS and PMMA are the materials presenting the most promising results for the desired application. However, further *in vitro* studies are required to confirm these results, namely, studying aging in artificial saliva.

3.2.3. Mechanical characterization

A protective mouthguard must present appropriate mechanical properties. Cummins et al. state that harder materials present a higher probability to effectively redistribute impact stresses and decrease their effects on the teeth-bone system [41]. In the present work, the σ and E values of the printed specimens were determined by three-point bending tests to evaluate the influence of layer height and total device thickness. The obtained results are plotted in Figs. 4 and 5. A table (Table S1) with the summary of the values of σ and E is presented in the supplementary information section.

The results obtained for rPLA agree with what was already reported in the literature [23]. Regarding E, the mean value does not vary significantly with the printing quality nor with the total thickness of the specimen. Even though rPLA shows higher σ and E values, this material is not the most adequate for the fabrication of mouthguards due to the variation of the mechanical properties induced by the recycling process.

The results for PMMA show that the bending strength is higher for the specimens with lower layer height that may be related to the interlayer cohesion between the printed layers. The NQ printed specimens are constituted by thinner layers printed on top of each other, and so, the volume shrinkage associated with the solidification process after printing is also lower, favoring the cohesion between layers [42]. It is noteworthy to mention that thinner layers mean that to achieve the same specimen dimension, more material will be required in NQ printing, diminishing the porosity between layers due to their flattening. Therefore, more secondary bonds are formed resulting in an overall increase of the cohesive force. This results in higher bending strengths of the NQ specimens [43]. Considering the total specimen thickness, it was observed that both NQ and LQ specimens with 2 mm have slightly higher bending strength when comparing with the 4 mm samples.

The Young's modulus of PMMA samples presents no significant differences for the values when considering different printing qualities and thickness. Herein, for the preparation of a mouthguard using PMMA, it would be advisable to print it in NQ (0.1 mm layer height) with a total thickness of 2 mm.

The bending strength values determined for HIPS specimens follow the same trend as observed for PMMA. As discussed above, the decrease of layer height favors interlayer cohesion and diminishes the porosity resulting in superior bending strength. The samples with the highest bending strength are the ones printed in NQ and 4 mm of total thickness. This polymer also revealed higher E values when compared with the other polymers. For the envisaged application, the 4 mm total thickness devices may not be the best choice since they can compromise comfort. Therefore, 2 mm NQ HIPS samples would be recommended.

From all the studied materials, TPU presents the lowest σ and E values, which is in agreement with the literature [44]. Although the

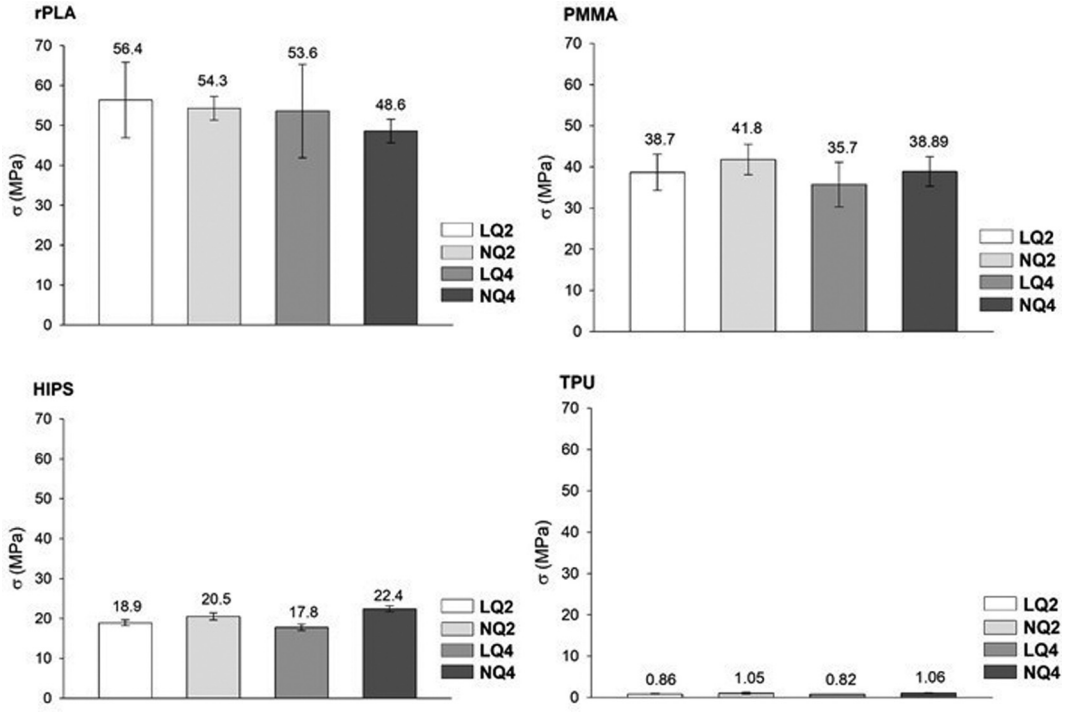

Fig. 4. Maximum bending stress value of the printed samples. The values are presented as Mean ± SD and the mean value presented.

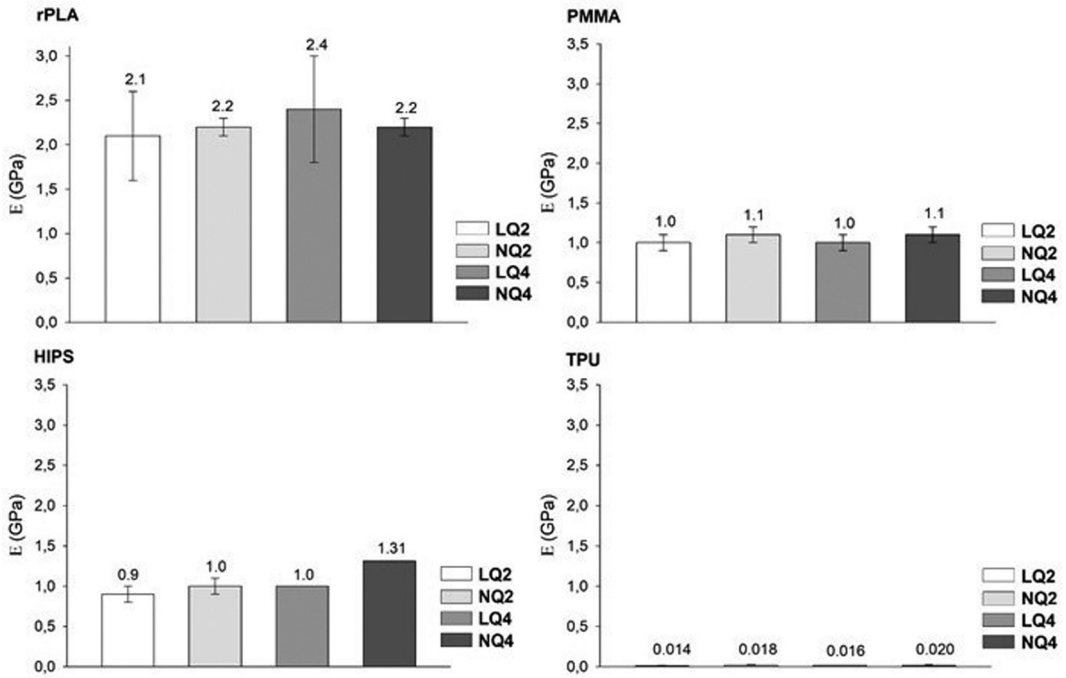

Fig. 5. Young's modulus of printed samples. The values are presented as Mean ± SD and the mean value presented.

differences between the values calculated for TPU and the other materials are not very big, results show that NQ specimens have higher bending strength. Similar to what was verified for PMMA and HIPS, with the decrease in layer height the cohesion between layers increases, resulting in a higher capability to resist the bending deformation, resulting in higher capability to resist to the bending deformation. On the other hand, the total thickness of the specimen does not significantly influence the bending strength of TPU samples. As expected, all

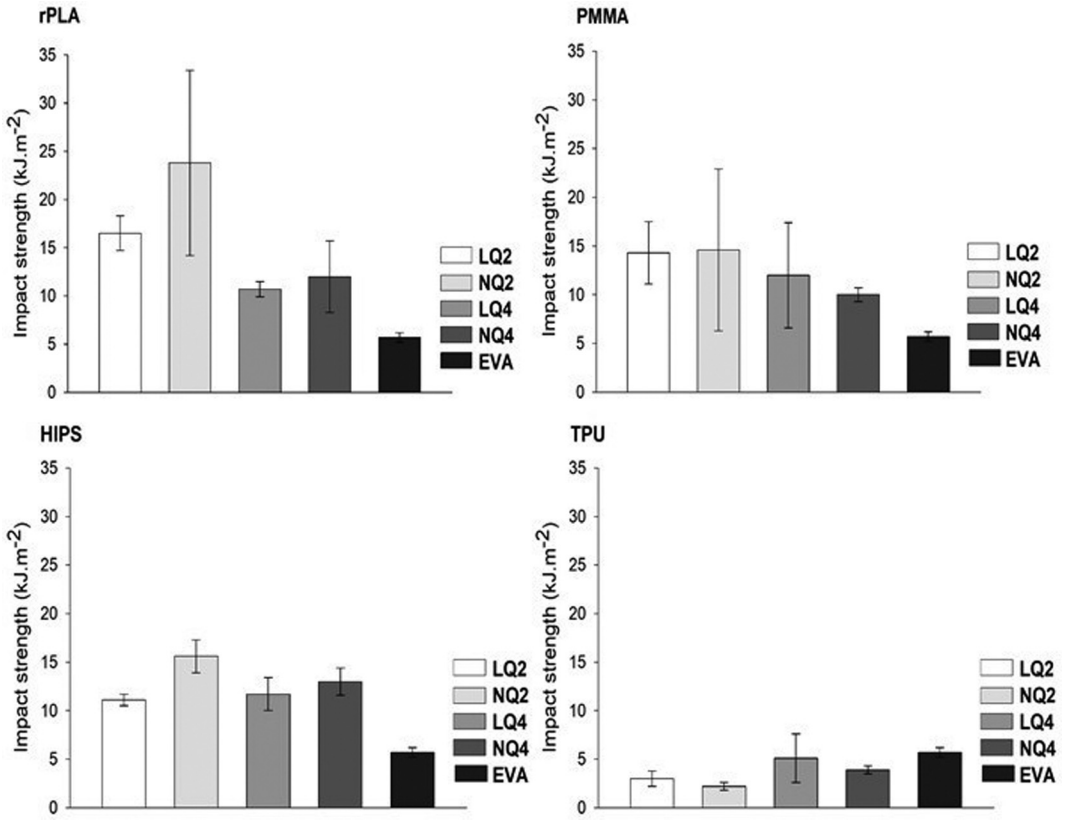

Fig. 6. Impact strength of the printed samples and EVA (control). Results are presented as Mean ± SD and the mean value presented.

TPU samples present the lowest *E* values of all materials studied. TPU, although considered a thermoplastic polymer, presents a mechanical behavior not too stiff and very similar to elastomers. As expected, Young's modulus of TPU is quite low and is not affected by the different parameters tested.

According to Gould et al., the base material of a mouthguard should not be too soft or too stiff and redistribute the shock tension by the largest area possible to reduce the load concentration in one specific point [45]. Consequently, PMMA and HIPS seem to be the most suitable candidates for mouthguards devices since both materials have higher bending strength than TPU and even than EVA, according to some reported studies [41].

The obtained results also indicate that a thickness of 2 mm may be sufficient for the redistribution of the impact energy. In order to confirm this assumption, transversal impact tests were performed.

The impact strength and absorbed energy were evaluated for the two printed qualities and thicknesses. EVA samples were studied as the control group, and the results are shown in Figs. 6 and 7 (Table S2).

The control material results show that EVA, 4 mm thick, present both low impact strength and low energy absorption. These results have opposite implications in the performance of the devices, as low impact strength implies that the material is more prone to fracture, whereas lower energy absorption protects the material from fracture. From the experimental data of the use of EVA, the energy absorption is mandatory, as there are no cases reported of fracture of EVA mouthguards. These observations suggest that evaluating a "perfect set" for the material properties is not straightforward.

The obtained results of impact strength for rPLA show that higher thickness implies lower impact strength while NQ printing presents, on average, higher values. As expected, with the decrease of layer height (NQ), the printed material becomes more compact, thus with an increased number of secondary bonds between layers, which implies that more energy is needed to fracture the specimen. The energy absorption does not vary significantly between the tested specimens, and only the LQ 2 mm shows a small decrease in the energy absorption.

Nonetheless, independent of the variable processing parameters, all rPLA specimens completely broke during the impact tests, and the produced damage in their morphology (supplementary information, Fig. S1 and S1A) is quite similar. When comparing with the control EVA copolymer, rPLA shows a higher absorbed energy percentage, which seems to be the reason why it completely fractures upon impact and EVA does not.

The tests with PMMA printed polymers produced similar results to what was observed for rPLA. The thinner specimens present higher impact strength, for the same reasons that have already been reported to rPLA. However, with PMMA, the thicker printed specimens, on average, slightly higher values of energy absorption were observed. After analysis of the images provided in the supplementary information (Fig. S2 and S2A), it is evident the delamination of the PMMA samples and the micrographs show that there are spaces between adjacent layers. Therefore, the apparently contradictory result where lower absorbed energy leads to the complete fracture of the material may be related to the lack of cohesion between layers. During the printing step, PMMA was the material processed at the lower ΔT between T_g and $T_{printing}$. Such implies a lower fluidity of the polymer during the printing process, with higher viscosity, less shape deformation after leaving the nozzle, and lower contact area and cohesion between adjacent layers of the final printed polymer.

The mean impact strength value of all the HIPS printed samples is very similar, with the NQ 2 mm presenting the highest value. Also, in this case, the increase in the number of secondary bonds can justify the observed increase. Moreover, the thinner specimens present lower energy absorption and, consequently, the ones with a set of mechanical properties more adequate for the fabrication of 3D printed

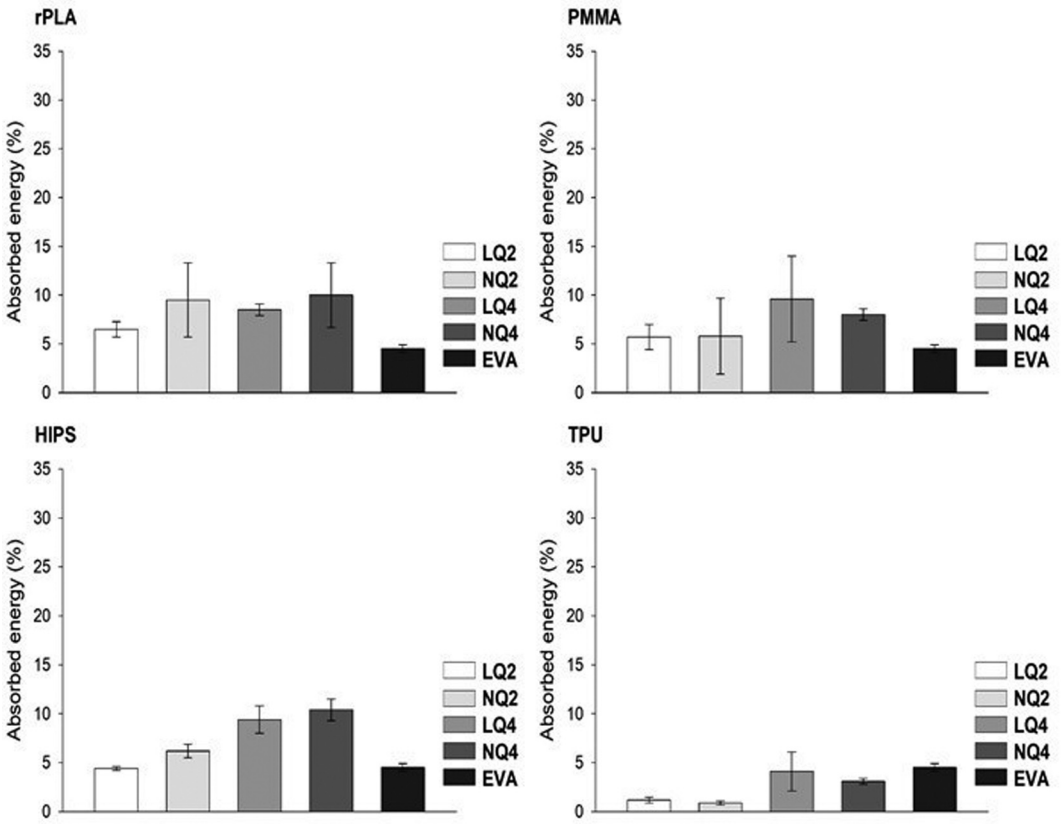

Fig. 7. Absorbed energy of the printed samples and EVA (control). Results are presented as Mean ± SD and the mean value presented.

mouthguards. The images of the morphology after the tests (Fig. S3) confirm these results as the 4 mm samples are the ones that show the most severe damage.

None of the TPU printed test samples suffered visible damage upon the transverse impact tests due to the elastomer-like behavior of TPU, already observed in the filament tensile tests. Both 4 mm bulk EVA and printed TPU show similar impact strength and absorbed energy percentage, which was expected according to already published results [10].

4. Conclusions

The study of different 3D printed polymeric materials as possible substitutes of EVA for mouthguards production was the principal motivation of the research described in this paper.

Surface characterization showed that all studied materials are hydrophobic with low surface energy, which indicates low water absorption and, consequently, no dimensional variation. Also, the reactivity with the oral cavity fluids is low, reducing the possibility of hydrolytic degradation and bacterial colonization.

The transverse impact test results highlighted that the ability to resist fracture is influenced by both the layer height (printing quality) and the total thickness of the specimen. In the present work, rPLA, PMMA, and HIPS present higher impact strength than TPU and EVA.

Another point worthy of consideration is the percentage of energy absorbed by the studied materials compared to EVA. Herein, 2 mm HIPS, 2 mm PMMA, and 4 mm TPU showed similar results to EVA. These results indicate that it could be viable to print a mouthguard of PMMA or HIPS with 2 mm thickness in NQ, as they are thinner and fulfill the required mechanical performance. Nonetheless, it is still necessary to find solutions that minimize the damage caused by impact. One possible strategy can be the combination of two different materials for the preparation of protective mouthguards. Due to the recycling process of rPLA and its influence on the mechanical properties, as future work, it would be interesting to consider only the combination of TPU with HIPS or PMMA.

CRediT authorship contribution statement

Ana M. Sousa: Investigation; Writing - original draft. **Ana C. Pinho**: Formal analysis; Supervision, Writing - review & editing. **Ana P. Piedade**: Writing - review & editing, Supervision, Project administration, Funding acquisition.

Declaration of Competing Interest

The authors declare that they have no known competing financial interests or personal relationships that could have appeared to influence the work reported in this paper.

Acknowledgements

This research was partially sponsored by FEDER funds through the program COMPETE2020– Programa Operacional Fatores de Competitividade –, Portugal2020 and by national funds through FCT – Fundação para a Ciência e Tecnologia -, under the projects UIDB/00285/2020, POCI-01-0145-FEDER-030767 and POCI-01-0247-FEDER-024533.

Appendix A. Supplementary data

Supplementary data to this article can be found online at https://doi.org/10.1016/j.matdes.2021.109624.

References

[1] M. Jegier, A. Smalc, A. Jegier, Selected dental concerns in sports medicine, Med. Sport. 9 (2005) 53–59.
[2] I. Zaman, S.A.M. Rozlan, B. Manshoor, M.Z. Ngali, A. Khalid, N.A.M. Amin, Study of Mouthguard Design for Endurance and air-Flow Intake, in: IOP Conf. Ser. Mater. Sci. Eng. Institute of Physics Publishing, 2017, 012007, https://doi.org/10.1088/1757-899X/226/1/012007.
[3] O. Lieger, T. Von Arx, Orofacial/cerebral injuries and the use of mouthguards by professional athletes in Switzerland, Dent. Traumatol. 22 (2006) 1–6, https://doi.org/10.1111/j.1600-9657.2006.00328.x.
[4] A.F.V.R. Queiróz, R.B. de Brito, J.C. Ramacciato, R.H.L. Motta, F.M. Flório, Influence of mouthguards on the physical performance of soccer players, Dent. Traumatol. 29 (2013) 450–454, https://doi.org/10.1111/edt.12026.
[5] K. Collares, M.B. Correa, I.C.M. da Silva, P.C. Hallal, F.F. Demarco, Effect of wearing mouthguards on the physical performance of soccer and futsal players: a randomized cross-over study, Dent. Traumatol. 30 (2014) 55–59, https://doi.org/10.1111/edt.12040.
[6] T. Von Arx, R. Flury, J. Tschan, W. Buergin, T. Geiser, Exercise capacity in athletes with mouthguards, Int. J. Sports Med. 29 (2008) 435–438, https://doi.org/10.1055/s-2007-965341.
[7] C.C. Gage, K.C.H. Bliven, R.C. Bay, J.S. Sturgill, J.H. Park, Effects of mouthguards on vertical dimension, muscle activation, and athlete preference: a prospective cross-sectional study, Gen. Dent. 63 (2015) 48–55 www.agd.org (accessed September 22, 2020).
[8] A.M. Sousa, A.C. Pinho, A. Messias, A.P. Piedade, Present status in polymeric mouthguards. A future area for additive manufacturing? Polymers (Basel) 12 (2020) 1–18, https://doi.org/10.3390/polym12071490.
[9] S.S. Mantri, S.P. Mantri, S. Deogade, A.S. Bhasin, Intra-oral mouth-guard in sport related oro-facial injuries: prevention is better than cure! J. Clin. Diagn. Res. 8 (2014) 299–302, https://doi.org/10.7860/JCDR/2014/6470.3872.
[10] D.R. Lunt, D.A. Mendel, W.A. Brantley, F. Michael Beck, S. Huja, S.D. Schriever, T.H. Grentzer, S.B. Alapati, Impact energy absorption of three mouthguard materials in three environments, Dent. Traumatol. (2010) 23–29, https://doi.org/10.1111/j.1600-9657.2009.00848.x.
[11] R. Karaganeva, S. Pinner, D. Tomlinson, A. Burden, R. Taylor, J. Yates, K. Winwood, Effect of mouthguard design on retention and potential issues arising with usability in sport, Dent. Traumatol. 35 (2019) 73–79, https://doi.org/10.1111/edt.12446.
[12] Y. Maeda, D. Kumamoto, K. Yagi, K. Ikebe, Effectiveness and fabrication of mouthguards, Dent. Traumatol. 25 (2009) 556–564, https://doi.org/10.1111/j.1600-9657.2009.00822.x.
[13] E.B. Tuna, E. Ozel, Factors affecting sports-related orofacial injuries and the importance of mouthguards, Sports Med. 44 (2014) 777–783, https://doi.org/10.1007/s40279-014-0167-9.
[14] S. Guérard, J.L. Barou, J. Petit, P. Poisson, Characterization of mouthguards: impact performance, Dent. Traumatol. 33 (2017) 281–287, https://doi.org/10.1111/edt.12329.
[15] J.L. Geary, M.J. Kinirons, Post thermoforming dimensional changes of ethylene vinyl acetate used in custom-made mouthguards for trauma prevention - a pilot study, Dent. Traumatol. 24 (2008) 350–355, https://doi.org/10.1111/j.1600-9657.2007.00550.x.
[16] C. Zamora-Olave, E. Willaert, L. Parera, N. Riera-Puñet, J. Martinez-Gomis, Experience with mouthguards and prevalence of orofacial injuries among field hockey players in Catalonia, Dent. Traumatol. 36 (2020) 285–290, https://doi.org/10.1111/edt.12531.
[17] D. Gawlak, E. Mierzwińska-Nastalska, K. Mańka-Malara, T. Kamiński, Assessment of custom and standard, self-adapted mouthguards in terms of comfort and users subjective impressions of their protective function, Dent. Traumatol. 31 (2015) 113–117, https://doi.org/10.1111/edt.12132.
[18] M.H. Almeida, G.V. Ceschim, N.L.P.P. Iorio, H.C.C. Póvoa, M.R.R. Cajazeira, G.S. Guimarães, L.S. Antunes, L.A.A. Antunes, Influence of thickness, color, and polishing process of ethylene-vinyl-acetate sheets on surface roughness and microorganism adhesion, Dent. Traumatol. 34 (2018) 51–57, https://doi.org/10.1111/edt.12374.
[19] P. Zhao, C. Rao, F. Gu, N. Sharmin, J. Fu, Close-looped recycling of polylactic acid used in 3D printing: an experimental investigation and life cycle assessment, J. Clean. Prod. 197 (2018) 1046–1055, https://doi.org/10.1016/j.jclepro.2018.06.275.
[20] A. Määttänen, A. Fallarero, J. Kujala, P. Ihalainen, P. Vuorela, J. Peltonen, Printed paper-based arrays as substrates for biofilm formation, AMB Express 4 (2014) 1–12, https://doi.org/10.1186/s13568-014-0032-0.
[21] A.C. Pinho, A.P. Piedade, Zeta potential, contact angles, and AFM imaging of protein conformation adsorbed on hybrid nanocomposite surfaces, ACS Appl. Mater. Interfaces 5 (2013) 8187–8194, https://doi.org/10.1021/am402302r.
[22] C. Jie-Rong, T. Wakida, Studies on the surface free energy and surface structure of PTFE film treated with low temperature plasma, J. Appl. Polym. Sci. 63 (1997) 1733–1739, https://doi.org/10.1002/(SICI)1097-4628(19970328)63:13<1733::AID-APP4>3.0.CO;2-H.
[23] A.C. Pinho, A.M. Amaro, A.P. Piedade, 3D printing goes greener: study of the properties of post-consumer recycled polymers for the manufacturing of engineering components, Waste Manag. 118 (2020) 426–434, https://doi.org/10.1016/j.wasman.2020.09.003.
[24] A. Kumar, T. Venkatappa Rao, S. Ray Chowdhury, S.V.S. Ramana Reddy, Compatibility confirmation and refinement of thermal and mechanical properties of poly (lactic acid)/poly (ethylene-co-glycidyl methacrylate) blend reinforced by hexagonal boron nitride, React. Funct. Polym. 117 (2017) 1–9, https://doi.org/10.1016/j.reactfunctpolym.2017.05.005.

[25] B.W. Chieng, N.A. Ibrahim, W.M.Z.W. Yunus, M.Z. Hussein, Poly(lactic acid)/poly (ethylene glycol) polymer nanocomposites: effects of graphene nanoplatelets, Polymers (Basel). 6 (2014) 93–104, https://doi.org/10.3390/polym6010093.
[26] R. Huszank, E. Szilágyi, Z. Szoboszlai, Z. Szikszai, Investigation of chemical changes in PMMA induced by 1.6 MeV He+ irradiation by ion beam analytical methods (RBS-ERDA) and infrared spectroscopy (ATR-FTIR), Nucl. Instruments Methods Phys. Res. Sect. B Beam Interact. Mater. Atoms. 450 (2019) 364–368, https://doi.org/10.1016/j.nimb.2018.05.016.
[27] A.C. Pinho, A.C. Fonseca, A.R. Caseiro, S.S. Pedrosa, I. Amorim, M.V. Branquinho, M. Domingos, A.C. Maurício, J.D. Santos, A.C. Serra, J.F.J. Coelho, Innovative tailor made dextran based membranes with excellent non-inflammatory response: In vivo assessment, Mater. Sci. Eng. C 107 (2020)https://doi.org/10.1016/j.msec.2019.110243.
[28] J. Coates, Interpretation of Infrared Spectra, A Practical Approach, in: Encycl. Anal. Chem. John Wiley & Sons, Ltd, Chichester, UK, 2006https://doi.org/10.1002/9780470027318.a5606.
[29] K. Hu, Z.K. Cui, Y. Yuan, Q. Zhuang, T. Wang, X. Liu, Z. Han, Synthesis, structure, and properties of high-impact polystyrene/octavinyl polyhedral oligomeric silsesquioxane nanocomposites, Polym. Compos. 37 (2016) 1049–1055, https://doi.org/10.1002/pc.23265.
[30] N.T. Thanh Truc, B.K. Lee, Combining ZnO/microwave treatment for changing wettability of WEEE styrene plastics (ABS and HIPS) and their selective separation by froth flotation, Appl. Surf. Sci. 420 (2017) 746–752, https://doi.org/10.1016/j.apsusc.2017.04.075.
[31] L. Jiang, Y. Jiang, J. Stiadle, X. Wang, L. Wang, Q. Li, C. Shen, S.L. Thibeault, L.S. Turng, Electrospun nanofibrous thermoplastic polyurethane/poly(glycerol sebacate) hybrid scaffolds for vocal fold tissue engineering applications, Mater. Sci. Eng. C 94 (2019) 740–749, https://doi.org/10.1016/j.msec.2018.10.027.
[32] Q. Tang, K. Gao, Structure analysis of polyether-based thermoplastic polyurethane elastomers by FTIR, 1H NMR and 13C NMR, Int. J. Polym. Anal. Charact. 22 (2017) 569–574, https://doi.org/10.1080/1023666X.2017.1312754.
[33] S. Wojtyła, P. Klama, T. Baran, Is 3D printing safe? Analysis of the thermal treatment of thermoplastics: ABS, PLA, PET, and nylon, J. Occup. Environ. Hyg. 14 (2017) D80–D85, https://doi.org/10.1080/15459624.2017.1285489.
[34] X.G. Zhao, K.J. Hwang, D. Lee, T. Kim, N. Kim, Enhanced mechanical properties of self-polymerized polydopamine-coated recycled PLA filament used in 3D printing, Appl. Surf. Sci. 441 (2018) 381–387, https://doi.org/10.1016/j.apsusc.2018.01.257.
[35] A.R. Prado, A.G. Leal-Junior, C. Marques, S. Leite, G.L. de Sena, L.C. Machado, A. Frizera, M.R.N. Ribeiro, M.J. Pontes, Polymethyl methacrylate (PMMA) recycling for the production of optical fiber sensor systems, Opt. Express 25 (2017) 30051, https://doi.org/10.1364/oe.25.030051.
[36] F. Vilaplana, A. Ribes-Greus, S. Karlsson, Analytical strategies for the quality assessment of recycled high-impact polystyrene: a combination of thermal analysis, vibrational spectroscopy, and chromatography, Anal. Chim. Acta 604 (2007) 18–28, https://doi.org/10.1016/j.aca.2007.04.046.
[37] X. Wang, H. Chen, C. Chen, H. Li, Chemical degradation of thermoplastic polyurethane for recycling polyether polyol, Fibers Polym. 12 (2011) 857–863, https://doi.org/10.1007/s12221-011-0857-y.
[38] M. Yahiaoui, J. Denape, J.Y. Paris, A.G. Ural, N. Alcalá, F.J. Martínez, Wear dynamics of a TPU/steel contact under reciprocal sliding, Wear. 315 (2014) 103–114, https://doi.org/10.1016/j.wear.2014.04.005.
[39] E.A. Vogler, Structure and reactivity of water at biomaterial surfaces, Adv. Colloid Interf. Sci. 74 (1998) 69–117, https://doi.org/10.1016/S0001-8686(97)00040-7.
[40] D. Geschke, Physical properties of polymers handbook, Zeitschrift Für Phys. Chemie. 199 (1997) 128, https://doi.org/10.1524/zpch.1997.199.part_1.128.
[41] N.K. Cummins, I.R. Spears, The effect of mouthguard design on stresses in the toothbone complex, Med. Sci. Sports Exerc. 34 (2002) 942–947, https://doi.org/10.1097/00005768-200206000-00006.
[42] W. Wu, P. Geng, G. Li, D. Zhao, H. Zhang, J. Zhao, Influence of layer thickness and raster angle on the mechanical properties of 3D-printed PEEK and a comparative mechanical study between PEEK and ABS, Materials (Basel). 8 (2015) 5834–5846, https://doi.org/10.3390/ma8095271.
[43] A. Farzadi, M. Solati-Hashjin, M. Asadi-Eydivand, N.A. Abu Osman, Effect of layer thickness and printing orientation on mechanical properties and dimensional accuracy of 3D printed porous samples for bone tissue engineering, PLoS One 9 (2014), e108252, https://doi.org/10.1371/journal.pone.0108252.
[44] K. Kim, J. Park, J. Hoon Suh, M. Kim, Y. Jeong, I. Park, 3D printing of multiaxial force sensors using carbon nanotube (CNT)/thermoplastic polyurethane (TPU) filaments, Sensors Actuators A Phys. 263 (2017) 493–500, https://doi.org/10.1016/j.sna.2017.07.020.
[45] T.E. Gould, M. Jesunathadas, S. Nazarenko, S.G. Piland, Mouth protection in sports, Mater. Sport. Equip. Elsevier 2019, pp. 191–231, https://doi.org/10.1016/B978-0-08-102582-6.00006-X.